Anal. Bioanal. Electrochem., Vol. 16, No. 7, 2024, 700-710
https://www.doi.org/10.22034/abec.2024.714700

Analytical & Bioanalytical Electrochemistry

2024 by CEE
www.abechem.com

Full Paper

Methyl p-toluenesulfonate as A Highly Effective Film-Forming Additive to Improve the Performance of A High-Voltage $LiMn_2O_4$ Cathode

Susan Hamidi,[1,2] Mehran Javanbakht,[1,2,*] and Mohammad Hassan Mousazadeh[1]

[1]*Department of Chemistry, Amirkabir University of Technology, Tehran 1599637111, Iran*
[2]*Renewable Energy Research Center, Amirkabir University of Technology, Tehran 1599637111, Iran*

*Corresponding Author, Tel.: +982164545806
E-Mail: mehranjavanbakht@gmail.com

Received: 14 May 2024 / Received in revised form: 9 July 2024 /
Accepted: 13 July 2024 / Published online: 31 July 2024

Abstract- The current study explores the film forming ability of a new additive Methyl p-toluene sulfonate (MPTS) on the $LiMn_2O_4$ (LMO) electrode and its effect on the electrochemical characteristics of lithium-ion battery. Based on the density functional theory analysis of the ionization energy (AIE) of MPTS and carbonate solvents, it was found that MPTS possesses the lowest AIE at 693.2 kJ/mol, suggesting a higher susceptibility to oxidation compared to the electrolyte solvents. Electrochemical and physicochemical analyses including linear sweep voltammetry, electrochemical impedance spectroscopy, field-emission scanning microscopy, indicated that the electrolyte with MPTS is prone to create a protective film with low impedance on the cathode electrode, which enhances the stability of the electrolyte and electrode upon battery cycling. The LMO/Li half-cell with 1.5% MPTS exhibits outstanding cyclic performance, retaining 90.53% of its capacity after 100 cycles, in comparison to 81.84% for the pristine electrolyte at high voltage. This improvement is because of the creation of a protective sulfur-containing layer on the cathode surface, which effectively prevents electrolyte degradation, reduces interfacial impedance, and enhances overall battery performance.

Keywords- Li-ion battery; Additives; Cathode Electrolyte Interphase (CEI); Sulfur-containing films; Theoretical calculations; Battery cycling

1. INTRODUCTION

Li-ion batteries have garnered significant attention as energy sources for various electronic and energy-storage devices, because of their numerous advantages over other types of batteries. These benefits encompass high energy density, eco-friendliness, and extended cycle longevity [1-4]. Lithium manganese oxide (LMO) has attracted much attention as a desirable cathode for LIB due to its outstanding features, like low toxicity, high operating voltage, good safety, and low expense. From the viewpoint of cyclic performance, LMO can't meet the commitment, so it is not extensively applied in the LIB industry. Generally, the main reason for poor cycling performance is that carbonate-based electrolytes undergo oxidation deterioration at high operating voltages giving rise to the interfacial impedance increment. Additionally, undesirable reactions between the electrolyte and electrode lead to the dissolution of Mn^{+2} ions into the electrolyte, which is deposited on the graphite electrode and damages its structure. Introducing an additive into the electrolyte with the ability to make an excellent protection film on the electrode sounds to be a cost-effective and facile way to meliorate the cycling stability of the battery [5,6]. Among different predominantly applied additives, Sulfur-based additives are the most widely accepted since they can considerably propagate the electrochemical performance of LIBs for extensive temperature ranges [7-9]. It should be noted that Sulfur atoms contribute to the construction of the cathode electrolyte interphase (CEI) film and generate ingredients such as $ROSO_2Li$ and $LiSO_3$, which are essential components of the protective film on a cathode. Moreover, using additives can emendate the SEI layers on electrodes and hinder the dissolution of Mn^{+2}, and also can prohibit electrolyte deterioration. Based on the literature, compounds containing S=O bond can serve as bifunctional electrolyte additives. This is because the sulfur in these materials is in an intermediate valence state, making it unstable and prone to both reduction and oxidation [10, 11]. Zheng et al. [12] have demonstrated that the oxidation activity of phenyl trifluoromethyl sulfide (PTS) is stronger than the carbonate-based electrolyte. As well as, they also found that PTS oxidizing sulfur contained radicals and fluorobenzene are generated and involved in the construction of a protective layer. According to researches done in the past, most studies have been concentrated on the film forming ability of sulfur-containing additives in the anode electrode. However, less consideration has been paid to LMO cathodes of the LIBs. Alternatively, achieving high performance in LIBs necessitates the creation of a stable and protective film on either the cathode or anode surface. In our previous work, we investigated film forming ability of MPTS on the graphite anode and we found that adding 1.5% MPTS in the pristine electrolyte can remarkably enhance the electrochemical performance of the Graphite/Li cell [13]. The present study investigates the impact of MPTS on the electrochemical performance of the LMO electrode. Density functional theory (DFT) calculation and linear sweep voltammetry illustrated that MPTS tends to be preferentially oxidized. Hence, it is anticipated that MPTS not only could create a SEI layer on the anode, but also it can be successful in generating a protective layer on the cathode. Charge–

discharge, linear sweep voltammetry (LSV), and electrochemical impedance spectroscopy (EIS) were performed to evaluate the electrochemical performance. The results showed that applying 1.5% of MPTS significantly enhances the capacity and cyclability of the LMO through forming the cathode electrolyte interphase (CEI) on the electrode.

2. EXPERIMENTAL SECTION

2.1. Materials and methods

Battery-grade lithium hexafluorophosphate ($LiPF_6$) was acquired from Exir Gmbh. Methyl p-toluenesulfonate (MPTS), Dimethyl carbonate (DMC), and Ethylene carbonate (EC) were obtained from Sigma Aldrich.

The pristine electrolyte (blank) was obtained by dissolving 1 M of $LiPF_6$ in a 50:50 (v/v) mixture of EC: DMC. The experimental electrolyte containing MPTS was prepared by dissolving 1.5 wt.% MPTS in the blank electrolyte and stirring it for 20 minutes. The electrolyte solutions were prepared inside a glove box filled with Ar (H_2O < 1 ppm). The H_2O content in the samples was distinguished using a Karl Fischer 831 Coulometer (Metrohm, Swiss) and was kept below 1 ppm. The LMO electrode was achieved by coating a mixture of 85 wt.% of $LiMn_2O_4$ powder, 10 wt.% of carbon black, and 5 wt.% polyvinylidene fluoride (PVDF) in N-methyl pyrrolidinone (NMP) on an aluminum foil and then, the obtained electrodes were further dried in a vacuum oven at 100 °C for 12 h. The 11 mm diameter electrode disc was then punched from the coated foil. Finally, the $LiMn_2O_4$/Li half-cells were assembled using Li metal as reference and counter electrodes and Celgard 2400 divider in a glovebox filled with Ar.

Electrochemical impedance spectroscopies (EIS) after 100 cycles at OCV were recorded by a Galvanostat/Potentiostat Autolab (PGSTAT 302N) with frequency varied from 0.1 Hz to 100 kHz and voltage amplitude of 5.0 mV. The LSV measurement was conducted between 3.0 and 6.0 V (vs Li/Li^+) at a scanning rate of 0.2 mV s^{-1} in a three-electrode configuration, using Li foil as the counter and reference electrodes, and a platinum electrode as the working electrode.

To explore the impact of MPTS on the cyclic stability of LMO, charge/discharge tests were conducted by a Neware eight-channel battery tester at room temperature. The LMO/Li half cells underwent charging to 4.5 V and discharging to 2.2 V at a rate of 0.2 C (1C= 120 mA h g^{-1}) for the initial two cycles. Subsequently, the cells were charged and discharged at 1 C for the remaining cycles within the same voltage range. The capacity retention is determined after representative cycles by assessing the capacity of the third cycle following the formation process. In addition, the C-rate capabilities were evaluated by varying the charge and discharge current densities from 0.2 C, 0.5 C, 1 C, 2 C, and finally returned to 0.2 C. In order to prepare cycled electrodes for physical characterization, the electrodes were disassembled in an Ar-filled glovebox, rinsed three times with dimethyl carbonate (DMC) to eliminate electrolyte residues, and then dried. The electrode morphology was observed using a field-emission

scanning electron microscope (FESEM, MIRA3), and an X-ray diffractometer (XRD, EQUINOX3000, Inel) was applied to analyze the crystalline structure of the electrode. The surface composition of cycled electrodes was evaluated by energy-dispersive X-ray spectroscopy (EDX) and elemental mapping.

2.2. Computational methods

Density functional theory (DFT) calculations were applied to evaluate the oxidation ability of the MPTS [14]. The energy of the highest occupied molecular orbital (HOMO) of the MPTS additive was calculated and compared with EC and DMC. The structures were optimized using the B3LYP method with a 6–311++G (d, p) basis set [13, 15]. Additionally, the polarized continuum model (PCM) as implemented in Gaussian 09 was used to account for the implicit solvent effect on the oxidation processes of MPTS[16]. The dielectric constant of 51.4, corresponding to an EC: DMC ratio of 50:50 was used for all PCM calculations.

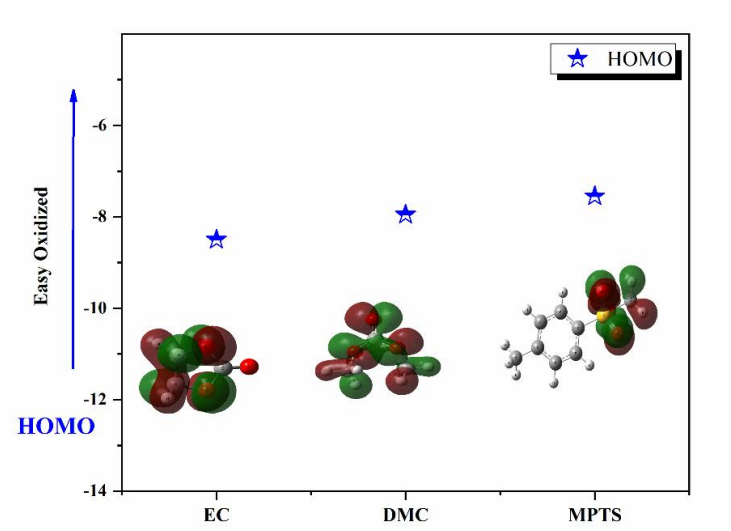

Figure 1. Optimized structures and HOMO energy of MPTS, EC, and DMC molecules

3. RESULTS AND DISCUSSION

3.1. DFT computations

To examine the electrochemical reactivity of MPTS, both theoretical calculations and electrochemical experiments were performed. According to the molecular orbital theory, the energy levels of HOMO and LUMO indicate the ability to accept or donate electrons [17-19]. Figure 1 illustrates the optimized structures of EC, DMC, MPTS, along with their respective HOMO energy levels. The MPTS additive has the highest HOMO energy (−7.55 eV) in comparison with the carbonate solvents. Suggesting that it is more prone to lose a valence electron to be oxidized prior to carbonate solvents [2,14,20]. To enhance our understanding of MPTS's oxidation activity, the ionization energy (AIE) was also calculated, yielding similar

results. According to the computed AIE shown in Figure 2, MPTS has the lowest AIE of 693.2 kJ/mol indicating MPTS is more likely to be oxidized than the solvents of electrolyte. This conclusion suggests that MPTS has higher electrochemical activity than electrolyte solvents, which could lead to the formation of a protective layer to inhibit electrolyte decomposition.

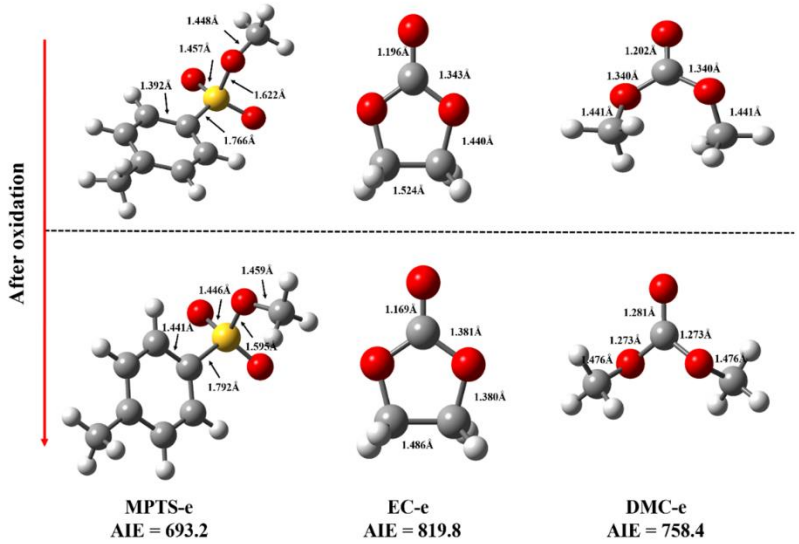

Figure 2. Optimized structures and ionization energy (AIE, KJ mol^{-1}) of MPTS, EC, and DMC before and after single-electron oxidation

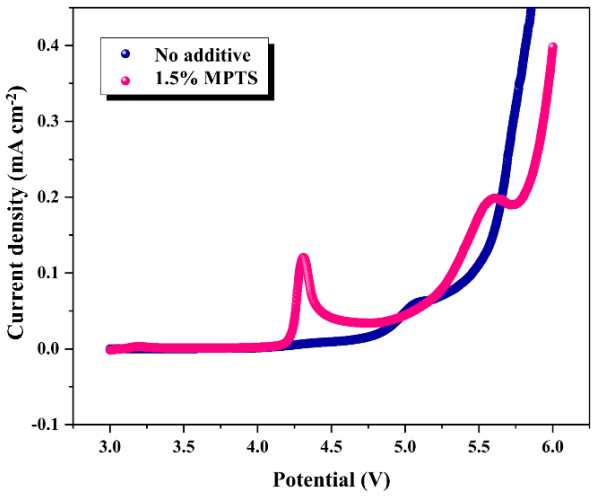

Figure 3. LSV curves of Pt electrodes in pristine and MPTS-containing electrolytes

3.2. Electrochemical performance of MPTS

The oxidative behavior of MPTS and MPTS-free electrolytes has been comparatively conducted via linear sweep voltammetry (LSV) with Pt electrode in a three-electrode cell. As depicted in Figure 3, the additive-free electrolyte decomposed at 5.0 V, where the current

sharply increased, while there is an obvious current peak around 4.2 V *vs.* Li/Li^+ in the electrolyte with 1.5 wt. % MPTS, representing that MPTS oxidized ahead of the electrolyte, and then the major ingredients decomposed at 5 V. The outcomes demonstrated that the MPTS can be preferentially oxidized and may take part in the construction of a protective film on the cathode electrode.

Figure 4(a) demonstrates the cycle-life performance of the LMO/Li half cells with and without MPTS. At first, the cells were cycled at 0.2 C for 2 cycles and 1 C for subsequent 100 cycles at room temperature. It can be understood that the cyclic stability and coulombic efficiency of LMO electrodes are enhanced by the inclusion of MPTS. The capacity retention of the cells in MPTS-free electrolyte and with 1.5% MPTS is 81.84% and 90.53% after 100 cycles respectively. The enhanced electrochemical behavior is likely due to the earlier oxidation reaction of MPTS, creating a passivation film on the electrode, which efficiently inhibits the additional degradation of the electrolyte on the surface of LMO. It should be noted here that HF production from hydrolysis and decomposition of $LiPF_6$ is important, which can expedite the dissolution of interfacial transition metals from LMO. The existence of transition metals in the electrolyte accelerates its decomposition and also co-intercalates into the anode structure which causes capacity fade. When a good protective layer is constructed on the cathode, the dissolution of transition metals is inhibited. Consequently, the decomposition of electrolytes may be repressed by film forming ability of MPTS on the cathode.

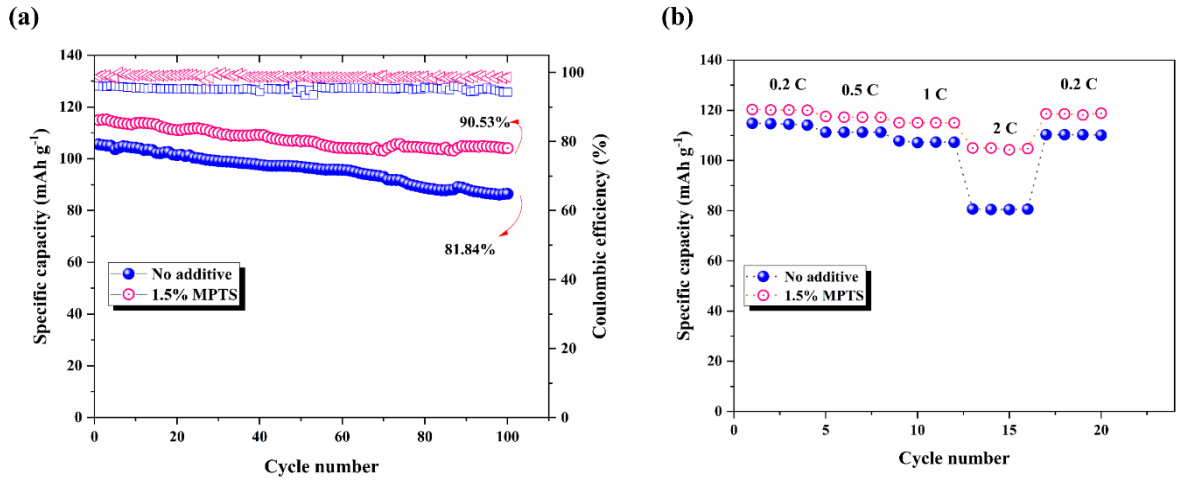

Figure 4. Cycling performance of LMO/Li half-cell in the potential rang of 2.2–4.5 V with and without MPTS additive (a): rate capability (b)

The rate capability of the LMO/Li cell was also assessed at 0.2 C, 0.5 C, 1 C, 2 C, and 0.2 C. Each current rate was evaluated over four cycles in both the additive-free electrolyte and MPTS-containing electrolyte. As depicted in Figure 4(b), the battery's discharge capacity in the electrolyte containing 1.5 wt% MPTS exhibits a notably higher discharge capacity

compared to the battery in the additive-free electrolyte. As the current density increases from 1 C to 2 C, the capacity in the electrolyte with 1.5 wt% MPTS decreases to approximately 104 mAh g^{-1}, indicating a capacity loss of 11 mAh g^{-1}. In contrast, the base electrolyte's discharge capacity falls sharply to ~80 mAh g^{-1}, with a capacity loss of 27 mAh g^{-1}. Moreover, when the rate is lowered back to 0.2 C, the electrolyte with MPTS shows a higher discharge capacity compared to blank electrolytes. In conclusion, the addition 1.5 wt% MPTS into the pristine electrolyte significantly enhances the rate capability of the LMO electrode, especially at current densities above 1 C.

To investigate further, electrochemical impedance spectra (EIS) were measured on LMO/Li cells after cycling in pristine and MPTS-containing electrolytes. The Nyquist plot in Figure 5 reveals two semicircles for both cells at low and medium frequencies, indicating charge transfer resistance (R_{CT}) and SEI film resistance (R_{SEI}) respectively. The cell without additive depicts a significant increase in total resistance, including both R_{CT} and R_{SEI} [15, 21-24]. Nevertheless, in the MPTS containing electrolytes, there are significantly smaller R_{CT} and R_{SEI} observed after cycling. This finding suggests that the CEI film generated by MPTS on the electrode surface exhibits a lower R_{CT} (86 Ω) at the electrode-electrolyte interface compared to the pristine electrolyte (230 Ω). This facilitates the movement of Li^+ ions, resulting in an improvement in the cycle performance. In conclusion, the inclusion of MPTS can significantly reduce the overall resistance of the cell by creating a protective and conductive CEI layer between the electrolyte and electrode.

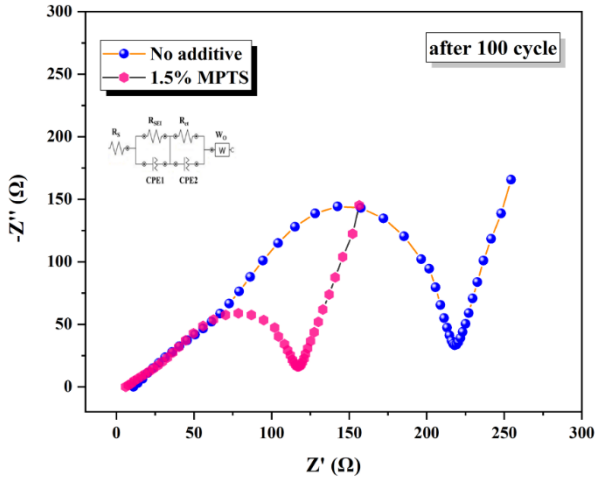

Figure 5. The EIS of LMO/Li in the electrolyte with and without MPTS after 100 cycles

Figure 6 displays the SEM images of the LMO surface before (fresh) and after cycling in both blank and MPTS-containing electrolytes along with EDS and mapping. The clean surface without any adducts is exhibited on the uncycled LMO electrode. While, thick electrolyte degradation adducts with a rough texture can be observed in the SEM images of cycled

electrode with additive-free electrolyte, which leads to a decrease in cyclic stability and capacity retention. By contrast, the cell with MPTS exhibited smooth and clean surface without cracking. The SEM images represent that MPTS creates a better CEI layer on the LMO electrode. Excessive electrolyte decomposition does not occur because the protective film covered the electrode surface. Hence, the use of MPTS considerably reduces the further degradation of the electrolyte and improves cyclic stability. Figure 6(g-j) shows the elemental mapping and EDS of LMO electrode after cycling in the additive-free electrolyte and with MPTS. The existing of the S element corroborates the film-forming reaction of MPTS. The EDS characterization further confirmed the existence of sulfur on the LMO surface after cycling in the electrolyte with MPTS.

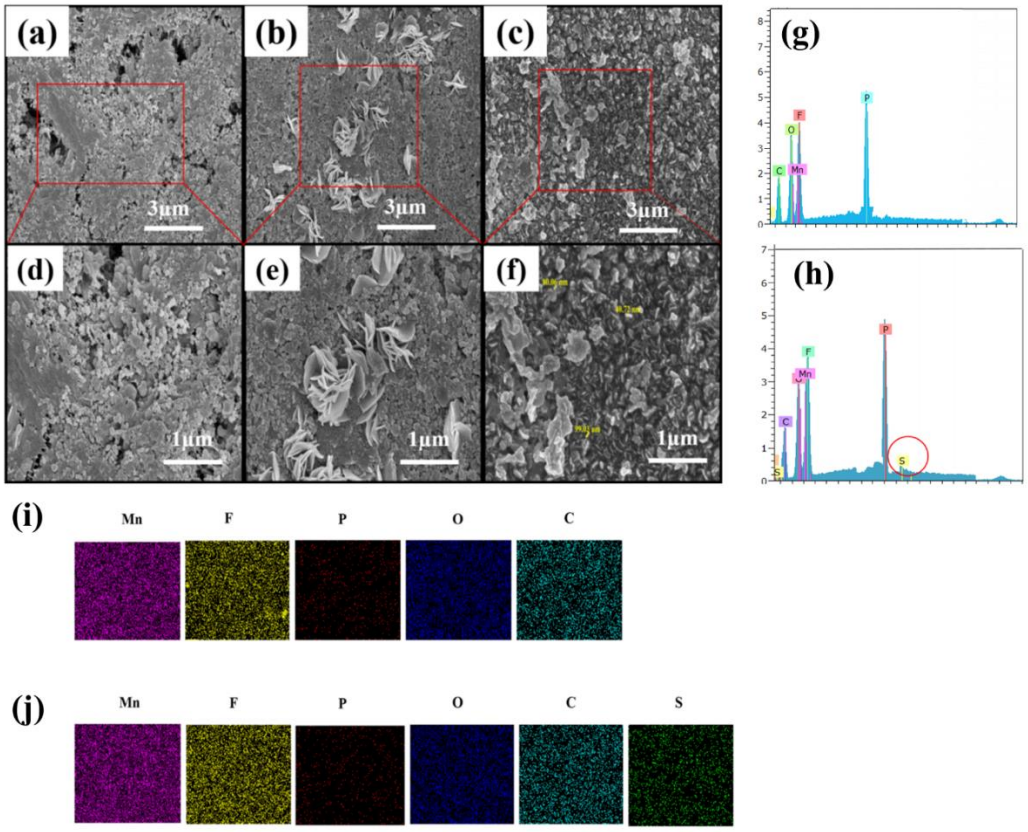

Figure 6. SEM images of LMO electrodes with a magnified view before (a, d); and after cycling in pristine electrolyte (b, e) electrolyte with 1.5% MPTS (c, f); Elemental mapping and EDX analysis of LMO cathodes after cycling in pristine electrolyte (i, g) and with 1.5% MPTS (j, h)

Figure 7 demonstrates the XRD spectrum of the fresh LMO electrode and LMO crystal structure after cycling in both blank and MPTS-containing electrolytes. As depicted in Figure 7, the XRD pattern of LMO cycled in an additive-free electrolyte reveals that the (111)

diffraction peak is weaker than that of fresh LMO, and the (311) and (400) peaks have vanished, indicating structural disintegration of LMO in the absence of additives. By contrast, $LiMn_2O_4$ after cycling with MPTS-containing electrolyte presents XRD patterns approximately similar to those of the fresh electrode which indicates the CEI created from MPTS enables adequate preservation for the crystal structure integrity. The outcome also matches with that seen by SEM.

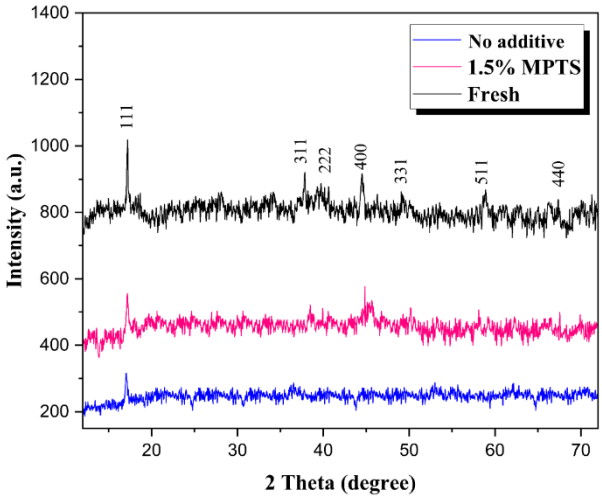

Figure 7. XRD patterns of the LMO cathode before and after cycling in the pristine and MPTS-containing electrolyte.

4. CONCLUSION

In this research, for the first time, MPTS is introduced as a new additive into LMO/Li cell operating at high voltage. Computational analysis using DFT revealed that MPTS undergoes preferentially decomposition through oxidation and contributes in the formation of the CEI layer. Furthermore, LSV, XRD, and SEM methods revealed that the preferential oxidation of MPTS results in the formation of a CEI layer that adheres to the cathode surface. This CEI layer proves beneficial in preventing electrolyte decomposition. The research revealed that the electrolyte containing 1.5 wt% MPTS shows improved cyclic stability at high voltage, maintaining 90.53 % of its capacity after 100 cycles, while the additive-free electrolyte retains only 81.84 %. This result suggests that MPTS could be a promising additive for forming a CEI layer in the high-voltage cathodes for Li-ion batteries. Such protective films are crucial for preserving the structural integrity of the LMO electrode.

Acknowledgments

The authors express their gratitude to Amirkabir University of Technology (Tehran, Iran) and the Renewable Energy Research Center (RERC) for their technical support of this work.

Declarations of interest

The authors declare no conflict of interest in this reported work.

REFERENCES

[1] S. Bolloju, C.Y. Chiou, T. Vikramaditya, and J.T. Lee, Electrochim. Acta 299 (2019) 663.
[2] Y. Che, X. Lin, L. Xing, X. Guan, R. Guo, G. Lan, Q. Zheng, W. Zhang, and W. Li, J. Energy Chem. 52 (2021) 361.
[3] Y. Lin, M. Xu, S. Wu, Y. Tian, Z. Cao, L. Xing, and W. Li, ACS Appl. Mater. Interfaces 10 (2018) 19.
[4] X. Yan, C. Chen, X. Zhu, L. Pan, X. Zhao, and L. Zhang, J. Power Sources 461 (2020) 228099.
[5] K. Wang, L. Xing, Y. Zhu, X. Zheng, D. Cai, and W. Li, J. Power Sources 342 (2017) 677.
[6] C. Wang, L. Ouyang, W. Fan, J. Liu, L. Yang, L. Yu, and M. Zhu, J. Alloys and Compounds 805 (2019) 757.
[7] T. Yang, W. Wang, S. Li, J. Lu, W. Fan, X. Zuo, and J. Nan, J. Power Sources 470 (2020) 228462.
[8] J. Xia, L. Ma, and J. Dahn, J. Power Sources 287 (2015) 377.
[9] S. Han, H. Zhang, C. Fan, W. Fan, and L. Yu, Solid State Ionics 337 (2019) 63.
[10] X. Zuo, X. Deng, X. Ma, J. Wu, H. Liang, and J. Nan, J. Mater. Chem. A 6 (2018) 30.
[11] D. Y. Wang, N. N. Sinha, J. C. Burns, R. Petibon, and J. R. Dahn, J. Power Sources 270 (2014) 68.
[12] X. Zheng, X. Wang, L. Xing, Y. Liao, M. Xu, X. Liu, and W. Li, Electrochim. Acta 352 (2020).
[13] S. Hamidi, M. Javanbakht, M.H. Mousazadeh, and S.S. Tafreshi, Ionics 30 (2024) 1.
[14] Y. Qian, Y. Kang, S. Hu, Q. Shi, Q. Chen, X. Tang, Y. Xiao, H. Zhao, G. Luo, K. Xu, and Y. Deng, ACS Appl. Mater. Interfaces 12 (2020) 9.
[15] T. Yang, W. Fan, C. Wang, Q. Lei, Z. Ma, L. Yu, X. Zuo, and J. Nan, ACS Appl. Mater. Interfaces 10 (2018) 37.
[16] S. Hamidi, M. Javanbakht, and M.H. Mousazadeh, J. Appl. Electrochem. (2024) https://doi.org/10.1007/s10800-024-02112-0.
[17] T. Huang, X. Zheng, Y. Pan, Q. Li, and M. Wu, ACS Appl. Mater. Interfaces 11 (2019) 30.
[18] J. Guo, J. Li, Z. Fan, J. Qiu, H. Ye, J. Liang, J. Liang, R. Zeng, and Y. Cai, ACS Appl. Energy Mater. 6 (2023) 4.
[19] T. J. Lee, J. Soon, S. Chae, J. H. Ryu, and S.M. Oh, ACS Appl. Mater. Interfaces 11 (2019) 12.

[20] Q. Liu, G. Yang, S. Liu, M. Han, Z. Wang, and L. Chen, ACS Appl Mater Interfaces, 11 (2019) 19.
[21] M. Zhao, X. Zuo, X. Ma, X. Xiao, L. Yu, and J. Nan, J. Power Sources 323 (2016).
[22] S. Wu, Y. Lin, L. Xing, G. Sun, H. Zhou, K. Xu, W. Fan, L. Yu, and W. Li, ACS Appl. Mater. Interfaces 11 (2019) 19.
[23] M. Jayachandran, H.A. Therese, and T. Vijayakumar, Surfaces and Interfaces 42 (2023) 103339.
[24] L. Zhang, J. Liu, W. Wang, D. Li, C. Wang, P. Wang, K. Zhu, and Z. Li, Materials Chemistry and Physics 260 (2021).